# Fast flow, dipolarization, and substorm evolution: Cluster/Double Star multipoint observations

**R. Nakamura, T. Takada, W. Baumjohann, M. Volwerk, T. L. Zhang, Y. Asano, A. Runov, Z. Vörös, E. Lucek, C. Carr, B. Klecker, H. Rème, and O. Amm**

**Abstract**: Fast flow and associated magnetic field disturbances are keys to understand the link between the neat-Earth tail and the inner magnetosphere, where the essential energy conversion processes take place during substorms. The four-point Cluster observation allows to investigate spatial structure and associated signature of dipolarization disturbances. With the launch of Double Star, simultaneous observations of the inner magnetosphere and the midtail took place in summer 2004 and 2005. Such a constellation of spacecraft allows us further to study the flow and dipolarization disturbance both in the local and the larger context. That is, by applying multi-point analysis techniques, the direction and speed of the propagation is determined within the Cluster tetrahedron and can then be compared with the global propagation of the disturbances using Double Star as well as relevant ionospheric disturbances. We discuss plasma sheet fast flow and dipolarization characteristics obtained from local as well as global multi-point observations during substorms.

*Key words:* fast flows, dipolarization, substorms, Cluster, Double Star.

## 1. Introduction

High-speed plasma flows in the near-Earth plasma sheet are considered to play a key role in flux and energy transport in the magnetotail and substorm dynamics. Cluster traversed the magnetotail covering regions Earthward of 19 $R_E$ since summer 2001. The four spacecraft observations enabled us to differentiate spatial from temporal disturbances and provided a chance to obtain essential parameters, such as current density or spatial scale of the flow and field disturbances. Since the launch of the two satellites of the Double Star Program (DSP), Cluster and DSP allow large-scale multi-point observations along the same local time sector. Such simultaneous observations of the inner magnetosphere and the near-Earth tail are essential in substorm studies because of the initial local onset and the subsequent global expansion of the disturbance. Particularly, how these two key regions are linked in terms of fast flow and magnetic field dipolarization is yet to be determined to understand the mechanism of the substorm development.

The two satellites of DSP, TC1 and TC2, were launched in December 2003 and TC2 in July 2004, respectively, providing another opportunity to study fast flows in a more global context. Particulary, TC1, which has an equatorial orbit with an apogee of 13 Earth radii, and Cluster, which has an orbital plane in the same local time sector, can have interesting configurations to study the large scale propagation of the disturbances. Figure 1 shows the Cluster and TC1 location when TC1 observed a dipolarization defined as: $\Delta\theta_B > 10$ within 5 min, where $\Delta\theta_B$ is the latitude angle of the magnetic field, and TC1 and Cluster were at the night side, $X < -6\ R_E$ and $|Y| < 10\ R_E$, between July and October 2004. There are mainly two types of Cluster-TC1 configuration which are useful to study: (1) Changes across the current sheet when Cluster observes dipolarization-associated signatures at the boundary of the plasma sheet or lobe, and (2) Radial propagation of the disturbances when Cluster was near the equatorial plane. In this paper, we will discuss events with the latter type of orbit configuration.

In the following, we first highlight an event study by [1] which shows two examples when Cluster observed dipolarizations and TC1 was located close to its apogee at the same local time. We then survey the relationship between fast flows observed at Cluster and the dipolarization observed at TC1 in a more statistical way. In this study we mainly use data obtained by the fluxgate magnetometer (FGM) experiment on Cluster [2] and on TC1 [3] and also refer to the ion flow data from the Composition and Distribution Function Analyser (CODIF) of the Cluster Ion Spectrometry (CIS) experiment [4] onboard Cluster and from the Hot Ion Analyser (HIA) instrument [5] onboard TC1.

## 2. Local and global propagation of substorm disturbances

In this section, we discuss two events when Cluster observed clear fast flows and TC1 was located near the same local time sector Earthward of Cluster. Both events were observed in the post-midnight sector but during quite different solar wind conditions: disturbed IMF and steady northward IMF. By performing a timing analysis the direction and the propagation speed

Received 18 May 2006.

**R. Nakamura, T. Takada, W. Baumjohann, M. Volwerk, T. L. Zhang, Y. Asano,[1] A. Runov, and Z. Vörös.** Space Research Institute, Austrian Academy of Sciences, Schmiedlstr. 6, A-8042, Graz, Austria.
**E. Lucek and C. Carr.** Imperial College, London, SW7 2BZ, UK
**B. Klecker.** Max-Planck-Institut für extraterrestrische Physik, Postf. 1312, Garching, D-85741, Germany
**H. Rème.** CESR/CNRS, 9 Ave. du Colonel Roche, B.P. 4346, F-31028 Toulouse Cedex 4, France
**O. Amm.** Finnish Meteorological Institute, P.O. Box 503, FIN - 00101, Helsinki, Finland

[1]Present Address: Tokyo Institute of Technology, Meguro, Japan. (from April, 2006)

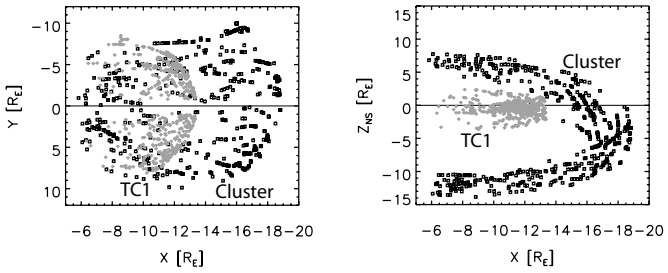


**Fig. 1.** Cluster and TC1 location plotted in the $X$-$Y$ plane (left) and in the $X$-$Z_{NS}$ plane (right), for those events when TC1 observed dipolarization and both spacecraft were at the night side, $X < -6\ R_E$, between July and October 2004. $Z_{NS}$ is $Z$ distances from the neutral sheet [6].

of the disturbance at Cluster were obtained and compared with the TC1 observations, which enabled to determine further constraints on the spatial and temporal profile of the sources based on these multi-distance multi-point observations with Cluster and TC1.

### 2.1. 20040807 event

Magnetotail data from Cluster and TC1, solar wind data from Geotail and ground magnetograms from selected MIRACLE stations ordered with increasing latitude are shown in Figure 2 adapted from [1]. Geotail was at $X = 15 \sim 17, Y = 1 \sim 7$, and $Z = 3R_E$ mainly in the solar wind except for short periods between 1915 and 2000 UT, indicated as shaded area in the figure, when the spacecraft entered into the magnetosheath. There were two intervals when IMF $B_Z$ was mainly negative with a minimum of $-5$ nT: 1845-2010 UT and 2105-2210 UT followed by a period of weak $B_Z$ with occasional short negative excursions until around 2245 UT when positive IMF $B_Z$ increased up to $+5$ nT and stayed northward for the following 45 min. Associated with the first negative IMF $B_Z$ interval, MIRACLE/IMAGE magnetograms detected an enhancement in westward electrojet activity starting at 2000, 2035 UT, and associated with the following negative IMF $B_Z$ interval, another onset at 2300 UT as indicated in the figure as vertical dotted lines. Corresponding to these westward electrojet activities, dispersionless injections were observed by LANL satellites at 1955-2000, 2032, 2247 and 2313 UT (not shown). These observations suggest that there were mainly two substorm intervals with multiple intensifications.

Associated with the first westward electrojet onset at 2000 UT little effects were seen at both spacecraft except for a gradual enhancement in the elevation angle in TC1. IMF $B_Z$ was still southward and $B_X$ at Cluster continued to increase ($\theta_B$ keeps decreasing) indicating further stretching of the field. On the other hand, the second westward electrojet at 2035 UT was accompanied by a clear change in the magnetic field configuration both at Cluster and TC1. Clear enhancement in $\theta_B$ was observed by Cluster, accompanied by a decrease in $B_X$, took place at 2033 and 2044 UT, which indicate a change from a tail-like to a dipolar configuration. TC1 was located in southern hemisphere as can be seen from the negative value of $B_X$ and also observed enhancements in $\theta_B$ accompanied by a decrease in the absolute value of $B_X$ starting at 2030 UT, and followed

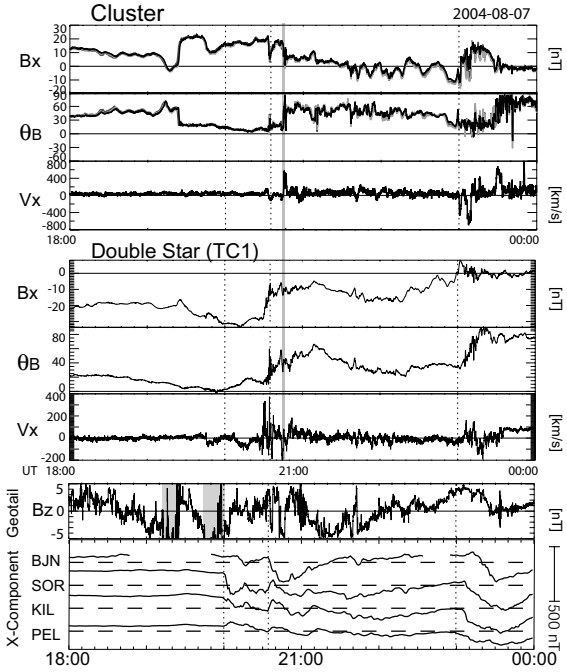


**Fig. 2.** Magnetotail data from Cluster and TC1, solar wind data from Geotail and ground magnetograms from selected MIRACLE stations (Adapted from [1]). Shown are $X$ components and latitude angle of the magnetic field and $X$ component of the proton flow from Cluster, $X$ component and latitude angle of the magnetic field and $X$ component of the ion flow from Double Star TC1, $X$ component of the magnetic field at Geotail in the solar wind and in the magnetosheath (shaded intervals), and $X$ component of the ground magnetogram from selected MIRACLE stations: BJN (CGM lat.71.45, CGM long. 108.07), SOR (67.34, 106.17), KIL (65.88, 103.79), PEL (63.55, 104.92) from the top to the bottom. The vertical dotted lines show the onset time of the enhanced westward electrojet, whereas the grey line indicates the dipolarization event discussed in the text in detail.

by a sharp increase in $\theta_B$ at 2034UT and 2042 UT. Fast Earthward ion bulk flows were detected at TC1 and Cluster starting at 2034 UT and 2044 UT, respectively. The reversal of the flow from tailward to Earthward was observed associated with 2300 UT onset by Cluster, while a clear dipolarization was observed at TC1. In the following we examine the temporal and spatial evolution of the dipolarization and flows at Cluster and TC1 in more detail for the dipolarization event at 2042-2044 UT marked with a grey line in the figure.

Figure 3 shows the $\theta_B$ profiles during the second dipolarization interval between 2040 and 2050 UT (left panel). To characterize the propagation of the dipolarization more quantitatively, we compared the local propagation properties of the $B_Z$ or $\theta_B$ disturbance among the four Cluster spacecraft with the larger scale propagation between Cluster and Double Star. We first determine the motion of the dipolarization signature from the timing analysis of Cluster, assuming the dipolarization front to be a planar structure. For the analysis we use the time difference of $\theta_B$ among the spacecraft for the events when clear enhancements were observed in $B_Z$ and $\theta_B$ and when all the Cluster spacecraft had similar profiles so that a

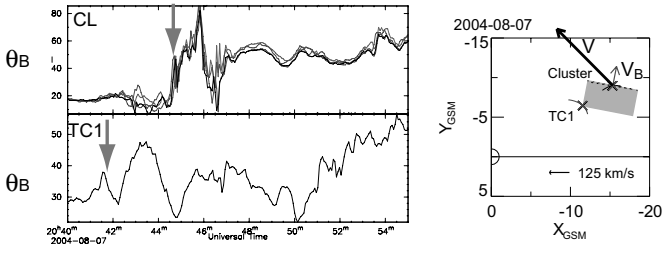


**Fig. 3.** Left: $\theta_B$ profiles during the second dipolarization interval between 2040 and 2050 UT observed by Cluster and TC1. The onset of Cluster dipolarization and the estimated onset of the TC1 from propagation speed at Cluster are indicated with arrows. Right: Location of Cluster and TC1 and direction of the fast flow (thick arrow) and propagation vector (thin arrow) of the dipolarization projected in the $X$-$Y$ plane.

timing analysis should be valid. Timing, propagation direction, and speed of dipolarization at Cluster are then compared with observed signatures at TC1. The propagation vector, $\mathbf{V}_B$, for this events is plotted in the right panel in Figure 3 with thin arrow. The propagation of the disturbances were mainly dawnward with a tailward component. This suggests that the initial source of the disturbance is located duskward and Earthward of Cluster toward the TC1 location. This procedure further allows to determine the arrival time of the disturbance at TC1, which can be expressed as $t_{TC1} = t_{CL} - ((\mathbf{R}_{CL} - \mathbf{R}_{TC1})\cdot \mathbf{V}_B)/(\mathbf{V}_B \cdot \mathbf{V}_B)$ assuming the spacecraft motion is negligible. Also we can determine the projected distance between Cluster and TC1 along this plane such as $|\mathbf{D}| = |\mathbf{R}_{CL} - \mathbf{R}_{TC1} - (t_{CL} - t_{TC1})\mathbf{V}_B|$. The dashed line perpendicular to the arrow in Figure 3 shows the projected components of displacement vector $\mathbf{D}$. Using this simple assumption, i.e., that the dipolarization is a planar front moving with a constant speed, we estimated that at TC1 the disturbance should take place at 2041 UT. For the 2041 UT event, this estimated timing is indicated with the thin arrow in the TC1 panel (bottom left) in Figure 3. TC1 in fact observed some enhancements in $\theta_B$ around 2042 UT. For this event, therefore, both spacecraft could likely have detected the same disturbances propagated from TC1 to Cluster and they were possibly related to the dipolarization front associated with Earthward flows. The propagation speed, $\sim 130$ km/s, was within the value of the previously obtained tailward propagation speed of 35-300 km/s [7, 8, 9]. Yet, the major direction was dawnward such as the case of dawnward expansion of the dipolarization observed in the post-midnight in the geosynchronous region [10]. The minimum required scale-size of the dipolarization disturbance then would have a width of 3.4 $R_E$, covering both TC1 and Cluster as shown with the hatched area in the right panel in Figure 3. Interesting to note that the propagation direction of the dipolarization is almost perpendicular to the main flow direction at Cluster, as indicated by the thicker arrow. It is therefore not the main flow direction in which the dipolarization front was observed to propagate. Such propagation of the dipolarization front predominantly perpendicular to the main fast flow direction was also reported by [11].

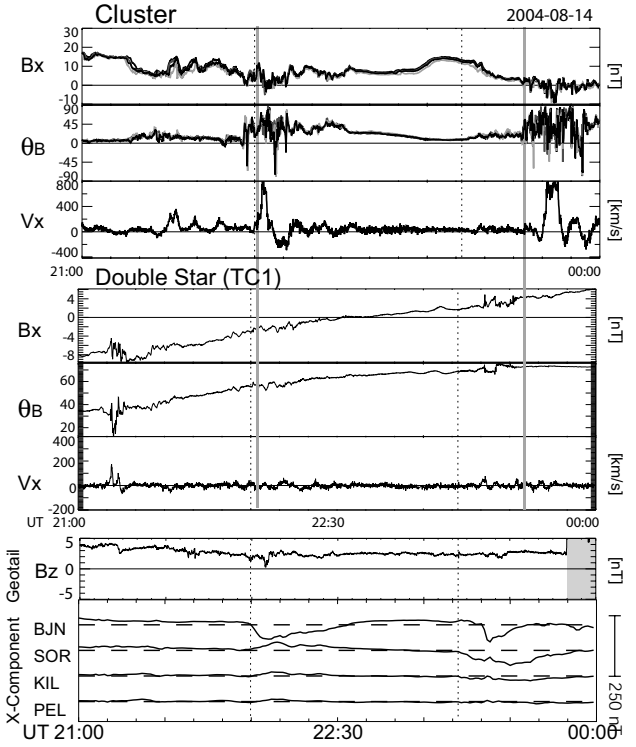


**Fig. 4.** Same as Figure 2 except for time interval between 21 and 24 UT, August 14, 2004 (Adapted from [1]).

### 2.2. 20040814 event

Figure 4 shows data from Cluster and Double Star TC1 together with the Geotail and MIRACLE magnetograms between 21 and 24 UT on August 14, 2004, in the same format as Figure 2. Geotail was located at $X = 8 \sim 9, Y = 29$, and $Z = -1 \sim -2R_E$, again mainly in the solar wind except for the magnetosheath encounter after 2350 UT. IMF $B_Z$ was all the time northward with a typical value of $\sim 3$ nT. Although weak, two westward electrojet disturbances can be identified in the MIRACLE magnetograms at 2157 UT and around 2312 UT, both centered at higher latitude than the previous event. No energetic particle injection was detected by LANL satellites (not shown). These signatures suggest a feature quite different from a usual "substorm", with disturbances mainly at high latitudes and equatorward propagation but not involving the inner magnetosphere. Cluster detected a sharp enhancement in $\theta_B$ followed by fast Earthward ion flow at 2156 UT and 2334 UT. The latter flow is almost 15 min delayed from the activation on the ground, although weak magnetic fluctuations started already after 2312 UT. On the other hand, TC1 showed no signature of clear dipolarization, but some magnetic disturbances after 2200 UT onset and after 2320 UT with no ion flow signature.

Similar to the previous event we examine the propagation of the Cluster disturbance and the flow disturbance. This will give us a hint of the maximum scale of the disturbance, not to be observed at TC1. The direction of the propagation of the dipolarization front was mainly Earthward/dawnward for the August 14 event as shown in Figure 5, deviating from the main

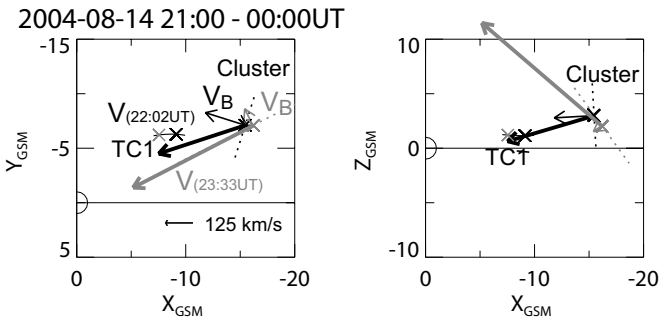


**Fig. 5.** Cluster and TC1 location in the $X$-$Y$ plane (left) and in the $X$-$Z$ (right) during the 2202 UT and 2233 UT events. The thick arrows show the flow direction while the thin arrows show the motion of the dipolarization front. The dashed lines show the possible spatial scale if it is assumed that the front also will encounter (or had encountered) TC1.

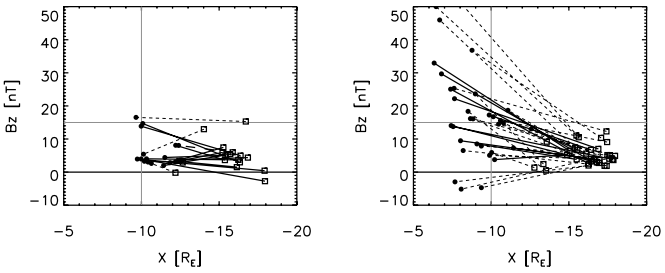


**Fig. 6.** $B_Z$ of Cluster and TC1 for the Cluster BBF events associated with TC1 dipolarization (left panel) and those without clear TC1 dipolarization (right panel) plotted against $X$ location of the two satellites. For $B_Z$ value at TC1, a 5-min average value before the dipolarization (left panel) or before Cluster BBF (right panel) are shown. The dashed (solid) lines indicate events when the two spacecraft were separated in $Y$ more (less) than 3 $R_E$.

flow direction. Similar Earthward/dawnward motion has been reported by Cluster in the postmidnight region associated with a BBF [11]. If we estimate the arrival time of the $B_Z$ enhancement at TC1, the 2202 UT and 2333 UT disturbances at Cluster are expected to be observed 3 min and 4 min later at TC1, when the scale size of the disturbance is larger than 3 and 8 $R_E$, respectively. The lack of such observations at TC1 suggests that the disturbance was either localized or decayed within a shorter time scale than these values. Either the BBF associated dipolarization was a transient phenomena and quenched between Cluster and TC1 or the localized BBF/dipolarization front could not be observed at TC1 resulting in only small magnetic field fluctuation. The lack of any injection signature at LANL as well as the location of the westward electrojet suggests that in fact the energy transported by the BBF is very likely dissipated mostly before reaching the TC1 region. On the other hand, the observation can be also due to the finite width of the flow channel, which was obtained to be 2-3 $R_E$ from a statistical study using Cluster multi-point dataset [12].

## 3. Survey of Cluster BBF and Double Star dipolarization

As shown in the previous sections, the evolution of a BBF can be quite different even though Cluster and TC1 were aligned in similar local time sectors. To determine the general condition of the fast flow evolution, we surveyed the dipolarization events in a more statistical manner. Here, we first created data base of Cluster bursty bulk flow events using data from Cluster 4 and TC1 dipolarization events. Bursty bulk flow events are defined when the spacecraft was in the plasma sheet (ion $\beta > 2$) and observed high speed flow ($V_{xy} > 300$ km/s) in the component perpendicular to the ambient field using 8 sec data. We take data points fulfilling the BBF condition separated less than 5 minutes as the same event. As for the dipolarization event, we used 5 minutes-long sliding windows of the spin-averaged data and identified a dipolarization when the difference between the minimum and maximum $\theta_B$ exceeds 10°. The event interval consists of consecutive intervals fulfilling this condition and its start time is defined as the time of minimum $\theta_B$ during the first interval and the end time is defined as the maximum $\theta_B$ during the last interval. We then examined whether such a dipolarization event is observed at TC1 associated with a Cluster BBF or not. That is, we divided the Cluster BBF dataset into two groups: those BBF events when there is TC1 dipolarization event within 5 min before or after the flow, which we call BBF event associated with dipolarization, and those BBF events when no corresponding TC1 dipolarization events can be found.

Figure 6 shows $B_Z$ of Cluster and TC1 for the Cluster BBF events associated with TC1 dipolarization (left) and those without clear TC1 dipolarization (right) plotted against the $X$ location of the two satellites during these events. For the $B_Z$ value at TC1, a 5-min average value before the dipolarization (left panel) or before the Cluster BBF (right panel) is shown. (Taking into account the near-Earth tail configuration, we actually used $H$ instead of $B_Z$ when TC1 is Earthward of 10 $R_E$). The dashed (solid) lines indicate events when the two spacecraft were separated in $Y$ more (less) than 3 $R_E$. It can be seen that when TC1 is located Earthward of 8 $R_E$ there is no clear dipolarization obtained by TC1 associated with a BBF at Cluster, even if the two spacecraft were close in $Y$. Another interesting difference between these two events are the $B_Z$ values at TC1, which is particular clear when we compare only those closely aligned in $Y$ (solid line) and if one compares TC1 values around $X = -10 \sim -12$ $R_E$ where events from both groups exist. It can be seem that $B_Z$ at TC1 is larger for those events when a dipolarization is not observed at TC1. Note that such difference were also seen between the two events shown in the previous section. Namely, $\theta_B$ was larger for the 2004-08-14 event, when no clear dipolarization was observed associated with the BBF, compared to the 2004-08-07 event, when a dipolarization was observed both at Cluster and TC1.

One plausible interpretation for these two types is illustrated in Figure 7. That is, a thin current sheet is developed reaching toward the inner magnetosphere when both flows in the near-Earth (Cluster) and dipolarization at ~10 $R_E$ region (TC1) are observed (upper panel in Figure 7). On the other hand, for the cases shown in the right panel in Figure 6 and the August 14 event, the ~10 $R_E$ region (TC1) is in a more dipolar configuration when the flow brakes beyond this region so that dipolar-

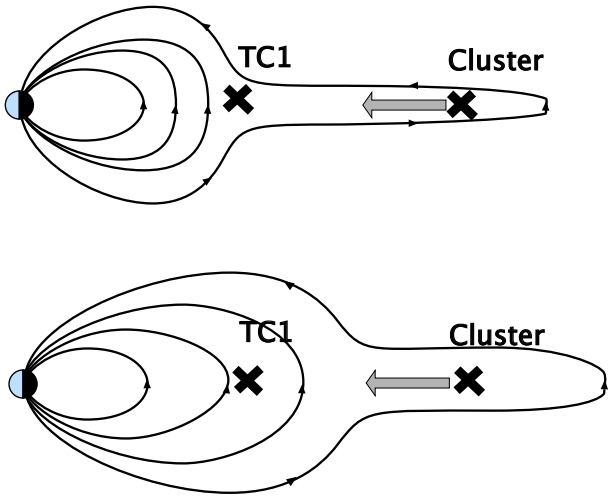


**Fig. 7.** Illustration of plausible tail configuration for events when TC1 observed dipolarization associated with Cluster BBF (upper panel) and those when TC1 observed no clear dipolarization (lower panel).

ization or flux pileup region cannot reach TC 1 region (bottom panel in Figure 7). More complete results of this statistical study will be published elsewhere (Takada et al., manuscript in preparation, 2006).

Note that we could not find any fast flow events associated with clear dipolarization signature in the geosynchronous region. This suggests that the fast flows most likely brakes radially outward than the geosynchronous region, which is also expected from the radial profile of the flux transport rate [13]. On the other hand, since there were no Cluster plasma sheet events when TC1 observed dipolarization in the geosynchronous distance, we have no supporting evidence that dipolarization at geosynchronous region can take place without flows in the near Earth region. Yet, the fact that there were no events with clear TC1 dipolarization at geosynchronous distance associated with Cluster fast flow in our dataset suggests that either a different process than flow braking or flux pile is needed for dipolarization near geosynchronous region or when a dipolarization takes place at geosynchronous region, the near-tail current sheet/plasma sheet is so thin that the chance of detecting plasma sheet flows with Cluster becomes almost zero. It is therefore essential to monitor the current sheet profile along an extended region in radial direction in order to determine the causal relationships between the fast flows and dipolarization. The THEMIS mission with spacecraft aligned in radial direction combined with geosynchronous satellites will be an ideal constellation to obtain a more conclusive answer.

## 4. Summary

Evolution of the fast flows and dipolarization is studied based on Cluster and Double Star TC1 satellite observations, which enabled large-scale multi-point observations along the same local time sector.

Two types of BBF events were introduced with different IMF conditions when Cluster and Double Star (TC1) were located in the same local time sector: August 7, 2004, 18-24 UT, during a disturbed southward/northward IMF interval, and August 14, 2004, 21-24 UT, when the IMF was stably northward. Cluster observed dipolarization as well as fast flows during both intervals, but this was not the case for TC1. By using multi-point analysis techniques, the direction/speed of the propagation is determined using Cluster and is then compared with the disturbances at TC1 to discuss its spatial/temporal scale. The propagation direction of the $B_Z$ disturbance at Cluster was mainly dawnward with a tailward component for August 7 and with a significant Earthward component for August 14 associated with fast flows. These differences suggest that the role of the BBF can be quite different for different IMF condition and resultant tail configurations.

By surveying Cluster BBF events when TC1 was in the tail, we could statistically confirm that there seems to be some difference in the tail configuration between these two types of BBF events. That is, a thin current sheet is most likely developed reaching toward the inner magnetosphere when both flows in the near-Earth tail (Cluster) and dipolarization in the $\sim$10 $R_E$ region (TC1) are observed. On the other hand, the $\sim$10 $R_E$ region (TC1) has likely a more dipolar configuration when there were no dipolarization observed by TC1 at this region associated with the fast flows in the near-Earth tail (Cluster). It should be also noted that we could not find any fast flow events associated with dipolarization when TC1 was near the geosynchronous region. That is, the observed flows most likely brake radially outward than the geosynchronous region. This suggests that either a different process than flow braking or flux pile is needed to explain a clear dipolarization at geosynchronous region or when a dipolarization takes place at geosynchronous region, the near-tail current sheet/plasma sheet is so thin that the chance of detecting plasma sheet flows with Cluster becomes almost zero.

These results show the complicated nature of the propagation of the disturbance in the tail and a new possibility of combining local and global multi-point analysis to further quantify the characteristics of the source regions.

## Acknowledgements

We acknowledge Z.-X. Liu and C. P. Escoubet for the successful Double Star program. We thank G. Laky for helping in the Cluster/Double Star data analysis, and T. Nagai for providing Geotail data. We acknowledge CDAWeb, WDC-C2, CSDS, GCDC, ACDC, CSSR, and EDDS for making available data used in this study. The work by M. Volwerk is financially supported by the German Bundesministerium für Bildung und Forschung and the Zentrum für Luft- und Raumfahrt under contract 50 OC 0104. A part of the work at IWF is supported by INTAS 03-51-3738 grant.

## References

1. Nakamura R., et al., Cluster and Double Star observations of dipolarization, *Ann. Geophys., 23*, 2915-2920, 2005.
2. Balogh, A., et al., The Cluster magnetic field investigation: overview of in-flight performance and initial results, *Ann. Geophys., 19*, 1207–1217, 2001.

3. Carr, C., et al., The Double Star Magnetic Field Investigation: instrument design, performance and highlights of the first years observations, *Ann. Geophys., 23*, 2713-2732, 2005.
4. Rème, H., et al., First multispacecraft ion measurements in and near the Earth's magnetosphere with the identical Cluster ion spectrometry (CIS) experiment, *Ann. Geophys., 19*, 1303-1354, 2001.
5. Rème, H., et al., The HIA instrument onboard the Tan Ce 1 Double Star near-equatorial spacecraft and its first results, *Ann. Geophys., 23*, 2757-2732, 2005.
6. Nakai, H., et al., Statistical nature of the magnetotail current in the near-Earth region, *J. Geophys. Res., 102*, 9573-9586, 1997.
7. Ohtani, S., et al., Radial expansion of the tail current disruption during substorms: a new approach to the substorm onset region, *J. Geophys. Res., 97*, 3129–3136, 1992.
8. Jacquey, C., et al., Tailward propating cross-tail current disruption and dynamics of near-Earth tail: A multi-point measurement analysis, *Geophys. Res. Lett., 20*, 983–986, 1993.
9. Baumjohann, et al., Substorm dipolarization and recovery, *J. Geophys. Res., 104*, 24995-25000, 1999.
10. Nagai, T., Observed magnetic substorm signatures at synchronous altitude, *J. Geophys. Res., 87*, 4405-4417, 1982.
11. Nakamura, R., et al., Motion of the dipolarization front during a flow burst event observed by Cluster, *Geophys. Res. Lett., 29*, 1942, doi:10.1029/2002GL015763, 2002.
12. Nakamura, R., et al., Spatial scale of high-speed flows in the plasma sheet observed by Cluster, *Geophys. Res. Lett., 31*, L09804, doi:10.1029/2004GL019558, 2004.
13. Schödel, R., et al., Rapid flux transport in the central plasma sheet, *J. Geophys. Res., 106*, 301, 2001.